Catal Lett (2009) 131:76–83
DOI 10.1007/s10562-009-9929-7

Abatement of Carbon Monoxide over CeO_2–CoO_x Catalysts: Effect of Preparation Method

Chih-Wei Tang · Chen-Bin Wang · Shu-Hua Chien

Received: 9 February 2009 / Accepted: 2 March 2009 / Published online: 17 March 2009

Abstract Four CeO_2–CoO_x catalysts (containing 20% ceria) were prepared by impregnation, precipitation-oxidation, co-precipitation and hydrothermal methods (IMP, PO, CP and HT, respectively). They were characterized by X-ray diffraction, high-resolution transmittance electron microscopy, N_2 adsorption–desorption, X-ray photoelectron spectroscopy, and temperature-programmed reduction. The catalysts catalyzed CO oxidation in a continuous flow micro-reactor. These results demonstrate that the activity of CO oxidation depended on both the surface area of catalyst and dispersion of ceria. The IMP catalyst exhibited substantial dispersion of CeO_2 on the surface of CoO_x and therefore the easiest release of oxygen to oxidize CO.

Keywords Cobaltic oxide · Ceria · CO oxidation

C.-W. Tang
Department of Chemical Engineering, Army Academy R.O.C., Taoyuan 32092, Taiwan, ROC

C.-B. Wang (✉)
Department of Applied Chemistry and Materials Science, Chung Cheng Institute of Technology, National Defense University, Tahsi, Taoyuan 33509, Taiwan, ROC
e-mail: chenbinwang@gmail.com; chenbin@ccit.edu.tw

S.-H. Chien
Institute of Chemistry, Academia Sinica, Taipei 11529, Taiwan, ROC

S.-H. Chien (✉)
Department of Chemistry, National Taiwan University, Taipei 10764, Taiwan, ROC
e-mail: chiensh@gate.sinica.edu.tw

1 Introduction

The design of novel catalysts of the abatement of carbon monoxide (CO) has become an important field of research in the last decade. This field of research has extensive applications in numerous areas such as vehicle exhaust catalysts [1], mine rescue devices [2] and catalytic combustion [3]. Both the noble metals and the transition metal oxides can catalyze the oxidation of CO. In particular, the catalytic performance of a gold catalyst depends on the particle size: smaller particles are more active in CO abatement at low temperature [4]. The high cost of precious metal has motivated an extensive search for alternative catalysts. As a single material catalyst, a transition metal is not as effective as a noble catalyst. Numerous composites have been applied to improve the catalytic activity toward CO oxidation. In recent years, much interest has been shown in the use of catalysts which contain binary or multiple metal oxides [5–11], such as, CoO_x/CeO_2 [5], CuO/CeO_2 [6], Co–Cu–Ce/γ–Al_2O_3 [7], Co_3O_4/Al_2O_3 [8], MoO_3/CeO_2 [9], CeO_2–ZrO_2 [10] and CuO/SnO_2 [11], all of which are effective in the oxidation of carbon monoxide. Interactions across the metal oxide interface have been suggested to be important, and carbon monoxide that is adsorbed on the metal reacts with the oxygen associated with the catalysts.

Among the metal oxides, cobalt oxide (Co_3O_4) is a particularly attractive material for catalyzing oxidation because of the presence of mobile oxygen in the surface [12–16]. The activity of Co_3O_4 toward oxidation is highly probable because of the relatively low ΔH of vaporization of O_2 [17, 18], and therefore demonstrates the relative weakness of the Co–O bond strength of Co_3O_4, which easily releases reactive oxygen species from the lattice. Cerium oxide (CeO_2) is an outstanding oxygen

ion-conducting material which has redox properties; it is therefore a good oxidation catalyst. Cerium oxide has been applied in the automotive three-way catalytic converter as an oxygen storage medium and stabilizer (such as in CeO_2–Al_2O_3 [1], CeO_2–SiO_2 [19], CeO_2–La_2O_3 [1] and CeO_2–HfO_2 [20]). Ceria performs numerous functions such as promoting CO oxidation, NO_x reduction; storing and releasing of oxygen and stabilizing the catalyst against sintering [21]. However, pure cerium oxide is rarely adopted as a catalyst due to its poor catalytic activity [22]. Modification with other transition metal oxides may increase stability at high temperature and improve its activity. Many methods can be used to prepare binary metal oxides, such as impregnation, co-precipitation and the sol–gel method and others.[14, 15, 23–28] Evaluating the activity of CO oxidation over Co_3O_4/CeO_2, Shen et al. [25] found that the catalyst prepared by the co-precipitation and oxidation prepared catalyst had the greatest catalytic activity. Also, in our earlier studies [27, 28] it was demonstrated that the CeO_2/Co_3O_4 catalyst has greater activity than other catalysts.

This work studies the effect of the method of preparation (such as impregnation, precipitation-oxidation, co-precipitation and the hydrothermal method) on the characteristics and catalytic properties of the CeO_2–CoO_x catalysts in the CO oxidation. The optimal ratio of CeO_2 to Co_3O_4 (containing 20% ceria), as determined elsewhere, is utilized. [27, 28] The catalysts are characterized by XRD, HRTEM, BET, XPS, and TPR. The results of the characterization and the catalytic activity are discussed in relation to the performance of the CeO_2–CoO_x catalysts.

2 Experimental

2.1 Preparation of Catalysts

Four methods were used to prepare CeO_2–CoO_x catalysts (containing 20% ceria)—IMP, PO, CP, and HT—for impregnation, precipitation-oxidation, co-precipitation and hydrothermal treatment, respectively. The precursors were $Ce(NO_3)_3 \cdot 6H_2O$ and $Co(NO_3)_3 \cdot 6H_2O$; the precipitant was NaOH and the oxidant was H_2O_2. The temperature of the hydrothermal process was 180 °C, which was maintained for 24 h. All as-prepared catalysts were dried at 110 °C and reduced in 10% H_2/Ar for 1 h at 200 °C.

2.2 Characterization of Catalysts

X-ray diffraction (XRD) measurements were made using a Siemens D5000 diffractometer with Cu $K\alpha_1$ radiation ($\lambda = 1.5405$ Å) at 40 kV and 30 mA with a scanning speed in 2θ of 2 min^{-1}. Diffraction peaks of the crystalline phase (Co_3O_4: 34-0394; CeO_2: 09-0418) were identified against standard compounds reported in the Joint Committee on Powder Diffraction Standards (JCPDS). The Scherrer equation yielded the crystallite sizes of cobaltic oxide and ceria.

The microstructures were characterized using transition emission microscopy and high resolution transition emission microscopy (TEM Hitachi H600-3 a 200 kV; HRTEM–JEOL JEM 2011). Samples were deposited by making an ethanol suspension on copper grids with a holey-carbon-film support. Magnification and CCD camera MSC SI0331 constants were calibrated using appropriate standards in the same electron-optical conditions.

Nitrogen adsorption isotherms at −196 °C were obtained volumetrically using a Micrometritics ASAP 2010. The catalysts were pre-outgassed at 5×10^{-5} Torr and 110 °C for 3 h. The surface area of the catalysts was determined from the nitrogen adsorption isotherm.

X-ray photoelectron spectra (XPS) were obtained using an energy analyzer with a constant pass energy of 20 eV followed by irradiaton of a catalyst pellet (6 mm in diameter) with a monochromatic Al K_α (1,486.6 eV) X-ray under ultrahigh vacuum conditions (1×10^{-10} Torr). Charging effects were corrected by adjusting the C1s peak to a position of 285.0 eV. The analysis of each catalyst began with a single-scan analysis of Co2p, Ce3d, C1s and O1s regions, in that order (for a total of 13 min), followed by a wide-scan analysis (5 min) at binding energies between 0 and 1,100 eV. The pass energy was set to 40 eV for wide-scan analyzes.

The reduction behavior of CeO_2–CoO_x catalysts was studied using temperature-programmed reduction (TPR). Approximately 25 mg of the catalyst was heated by using 10% H_2/N_2 gas mixture at a flow rate 10 mL min^{-1}. During TPR, the temperature was programmed to rise from 30 to 550 °C at 10 °C min^{-1}.

2.3 Measurement of Catalytic Activity

The catalytic activities of CeO_2–CoO_x catalysts in the oxidation of CO were measured in a continuous flow micro-reactor. A mixture of 10% O_2/He with 4% CO/He reaction gas was fed to a 0.5 g catalyst at a rate of 20 mL min^{-1}. Steady-state catalytic activity was measured at each temperature, as the reaction temperature was increased from room temperature to 200 °C in steps of 25 °C. The effluent gas was analyzed on-line using a Varian 3700 gas chromatograph with a carbosphere column. Before the reaction, the catalyst was pretreated by using 10% O_2/He at 110 °C for 1 h to drive away molecules that had been pre-adsorbed from the atmosphere.

3 Results and Discussion

3.1 Structural Characterization

The third column of Table 1 presents the BET specific surface area of the CeO_2–CoO_x catalysts. Both IMP and PO catalysts have a larger surface area (over 100 $m^2\ g^{-1}$) than CP and HT catalysts (below 90 $m^2\ g^{-1}$). Figure 1 presents the XRD patterns of CeO_2, Co_3O_4 and CeO_2–CoO_x catalysts. The diffraction patterns of CeO_2 obtained are 28, 47, and 57° (Fig. 1a) and reveal an fcc fluorite oxide-type structure. The IMP and PO catalysts (Fig. 1c, d) yield rather broad diffraction patterns, indicating the presence of a smaller crystallite, consistent with the fact that these catalysts have a higher specific surface area than the CP and HT catalysts (Fig. 1e, f). The XRD patterns of the IMP and PO catalysts include CeO_2, CoO and Co_3O_4 patterns, revealing that the ceria phase is highly dispersed on the cobalt oxide. The CP and HT catalysts exhibit only CeO_2 and Co_3O_4 patterns but not CoO patterns. Moreover, the Co_3O_4 pattern has stronger reflection peaks than obtained from either the IMP or PO catalyst. A comparison with the TEM images of the IMP and PO catalysts (Fig. 2a, b) reveals a highly dispersed morphology. The TEM images of CP and HT catalysts (Fig. 2c, d) have the hexagonal morphology of larger particles. To gain further insight into the microstructural characteristics of the CeO_2–CoO_x catalysts, HRTEM analyses are performed to distinguish the relative pattern of the species (Fig. 3). All samples displayed the three lattice fringe patterns, which corresponds to Co_3O_4 [lattice fringe at 4.6 Å for (111) plane], CoO [lattice fringe at 2.1 Å for (200) plane] and CeO_2 [lattice fringe at 2.70 Å for (200) plane]. Comparison with the XRD diffraction peaks, the absence of CoO phase on the PO and CP catalysts, was due to the overlap with Co_3O_4 pattern when 2θ reached 35°.

3.2 X-ray Photoelectron Spectroscopy

Figure 4 presents the XPS spectra of Co_{2p} of CeO_2–CoO_x catalysts. The peak of the $Co_{2p3/2}$ binding energy (BE) of all of catalysts is at 779.5–780.2 eV, which matches the reference values for Co_3O_4 (779.5 eV) and CoO (780.5 eV) [29, 30], respectively. Also, Kang et al. [5] obtained XPS spectra from CoO_x/CeO_2 catalysts and suggested that the interaction of metal oxide could change the electronic state of the cobalt and enhance its catalytic activity by the combined effect of cobalt oxide and ceria. The last two columns in Table 2 present the BE of $Co_{2p3/2}$ and the normalized peak area for Ce_{3d}. The BE of the $Co_{2p3/2}$ level of both IMP and PO catalysts is slightly shifted upward to ~780.2 and 780.0 eV, respectively. Figure 5 presents the XPS spectra of the Ce_{3d} of CeO_2–CoO_x catalysts. All catalysts yield six peaks at 880–920 eV. Based on XPS analyses, Mullins et al. [31] and Burroughs et al. [32] of CeO_2 with XPS, the $3d_{3/2}$ and $3d_{5/2}$ spin-orbit components associated with three pairs of spin-orbit doublets are designated U (U′, U″ and U‴) and V (V′, V″ and V‴), respectively. The IMP catalyst yields a more intense peak of XPS profile than the other catalysts. The XPS results show that Ce ratios of surface on the IMP, PO, CP and HT catalysts were 21:5:5:4, respectively. Combining these analyses with the quantitative analysis of surface components (Ce, Co and O, given in the fifth to seventh columns in Table 2), reveal the uniformed dispersion of a large amount of ceria on the surface of the

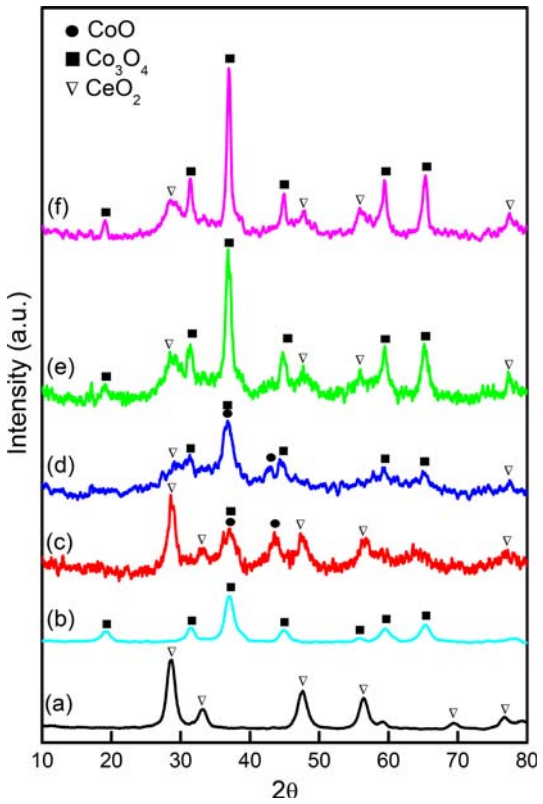

Fig. 1 XRD patterns of CeO_2–CoO_x catalysts: **a** CeO_2 **b** Co_3O_4 **c** IMP **d** PO **e** CP **f** HT

Table 1 Characterization and CO oxidation of CeO_2–CoO_x samples

Sample	Component[a]	S_{BET} ($m^2\ g^{-1}$)	TPR (°C)[b]		T_{50}^c
			α	β	
IMP	CeO_2, Co_3O_4, CoO	109	260	360	88
PO	CeO_2, Co_3O_4, CoO	140	283	485	93
CP	CeO_2, Co_3O_4, CoO	80	295	520	103
HT	CeO_2, Co_3O_4, CoO	87	300	375	119

[a] Characterized from XRD data

[b] Co_3O_4 was measured for TPR

[c] Temperature for 50% CO conversion

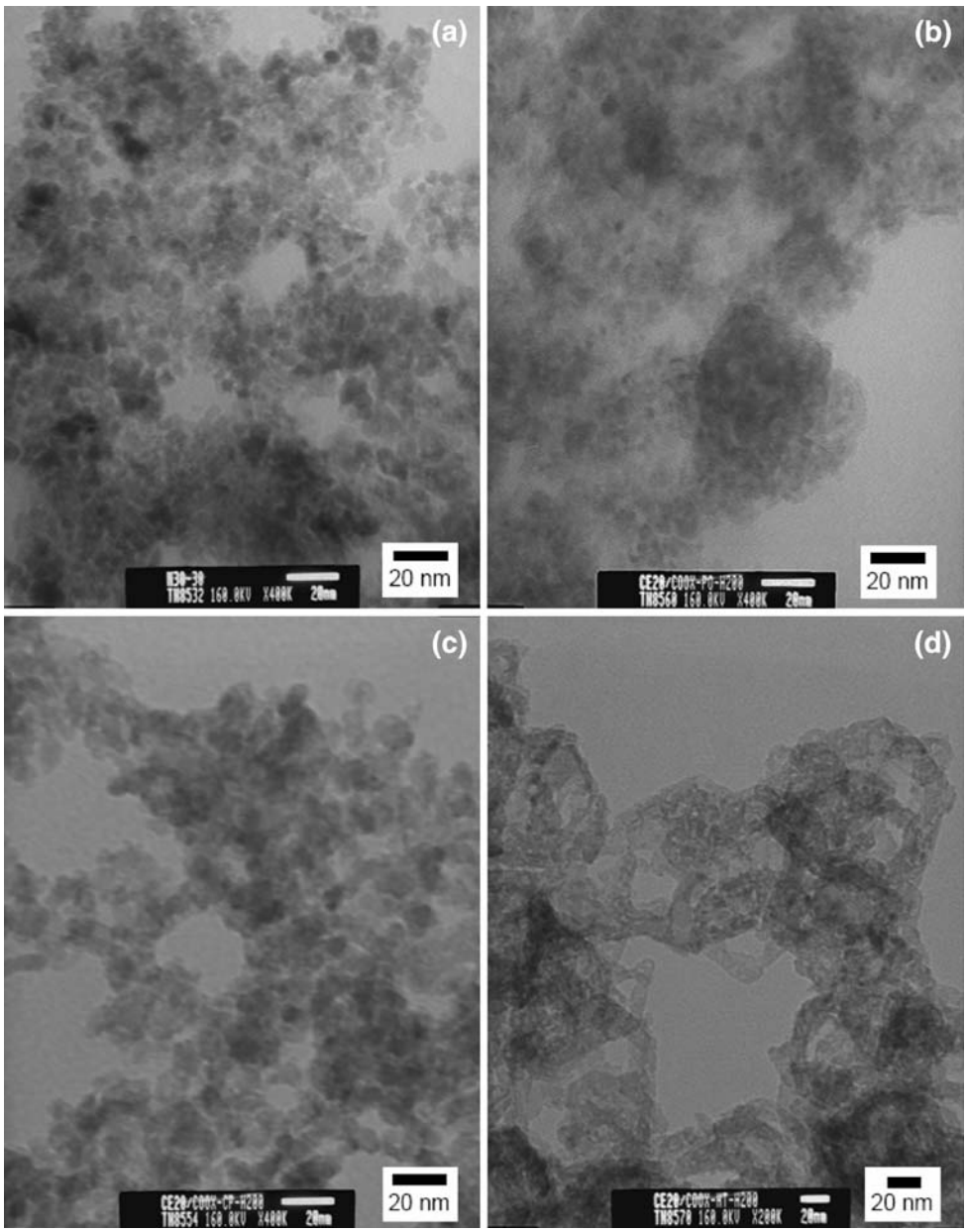

Fig. 2 TEM images of CeO_2–CoO_x catalysts: **a** IMP **b** PO **c** CP **d** HT

cobalt oxide of the IMP catalyst. Other preparation methods can lead some ceria into the bulk of catalysts; therefore the impregnation method can control the surface ratio of catalyst. Further the comparison of the TEM–EDX results for the components of all catalysts (second to fourth columns in Table 2), the Ce ratios are closely grouped near 20%. So we can distinguish the various ratios on surface and bulk of catalysts to affect the properties.

3.3 Temperature Program Reduction

To determine the Co–O bond strength in the CeO_2–CoO_x catalysts, the temperature program reduction (TPR) technique is used to elucidate the reduction behavior of these catalysts. Figure 6 shows the TPR profiles of the prepared CeO_2–CoO_x catalysts and the physically mixed catalyst (PM). All of the catalysts yield two sequent reduction peaks that comprise a low-temperature peak and a high-temperature peak (α and β peaks; the reduction temperatures are given in the fourth and fifth columns in Table 1). This reduction behavior is characteristic of the Co_3O_4 [27, 33, 34]. The first peak (α peak), of less intensity, appears at a lower temperature and overlaps with the more intense peak (β peak). According to the TPR results the α peak is due to the reduction of Co^{3+} to Co^{2+} and the β peak is due to the reduction of Co^{2+} to Co metal.

Comparing the effect of the amount of ceria on the surface of cobalt oxide (the fifth column in Table 2) with the

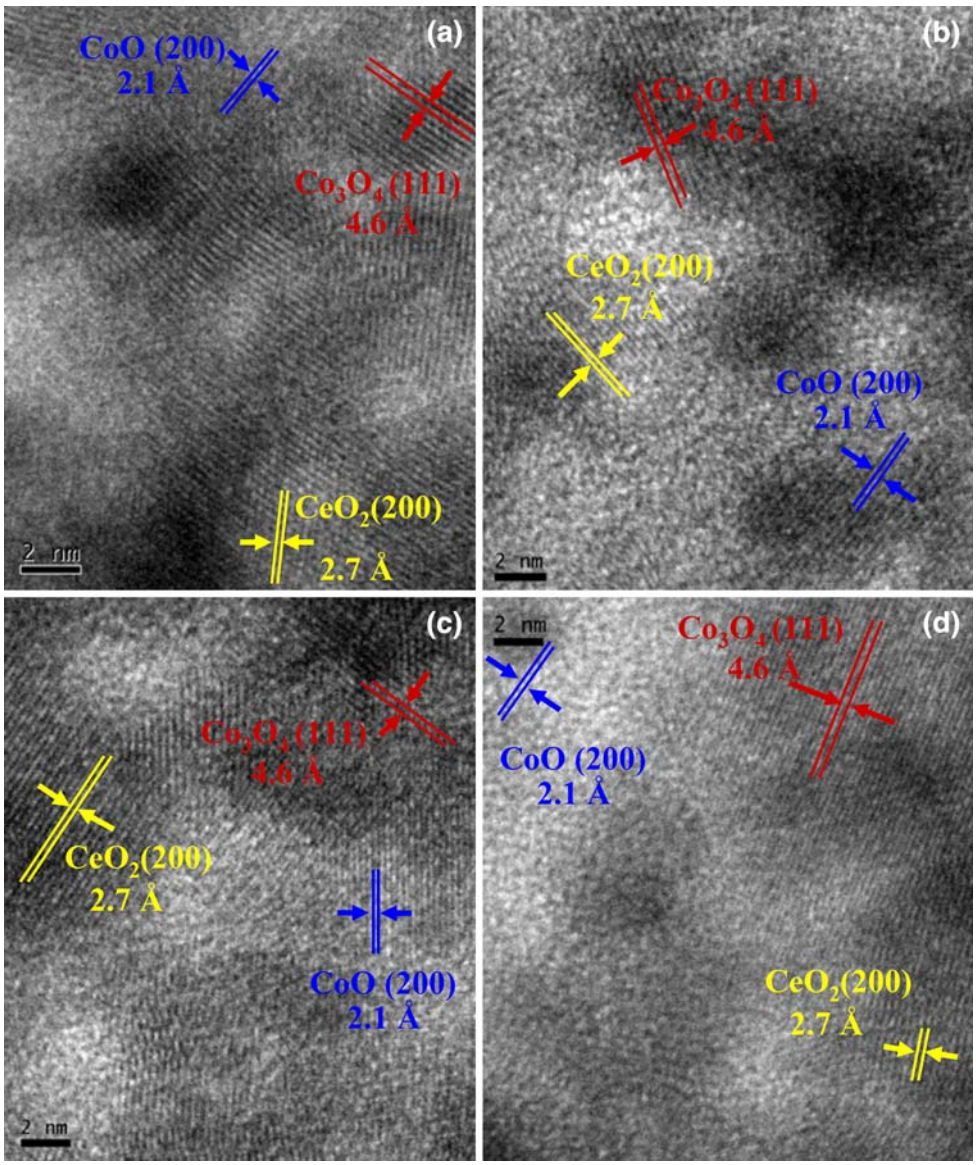

Fig. 3 HRTEM images of CeO_2–CoO_x catalysts: **a** IMP **b** PO **c** CP **d** HT

reduction behavior reveals an apparent shift in the α and β peaks. Both peaks shift to lower temperatures as the amount of ceria on the surface is increased: 260 and 360 °C for the IMP catalyst (surface content of ceria = 21%), and 300 and 375 °C for the HT catalyst (surface content of ceria = 4%), respectively. According to our previous studies [27, 28] that involved different ceria loadings (amounts = 4, 12, 20, 35, 50%) of the catalysts, the optimal loading (20%) is associated with the highest catalytic activity of CO. Therefore, optimal ceria content on the surface of the catalyst can weaken the bond strength of Co–O and promote the desorption of lattice oxygen from Co_3O_4, reducing the reduction temperature. Pure CeO_2 yields two reduction peaks at around 500 and 900 °C, which are attributed to the reduction of the surface and bulk oxygen of CeO_2, respectively [26, 35]. Additionally, the tailing β peak of TPR profile from the CeO_2–CoO_x catalysts (Fig. 6b–e) is attributed to the spillover of hydrogen from Co_3O_4 which promotes the reduction of the capping oxygen of ceria, whereas the PM catalyst (Fig. 6a) does not yield the tailing β peak. The shift in the reduction temperatures and tailing β peak behavior, associated with the combination of Co_3O_4 and CeO_2, is further evidence of combined effect. According to the difference of β peak on TPR profiles, we can distinguish two kinds of bond strength one which was strong and other one was weak. The IMP catalyst belongs to the weak bond strength due to the uniform dispersion. Both the PO and CP catalysts belong to the strong bond strength due to some cerium in the bulk. While, the HT catalyst possesses two kinds of strength since the preparation condition is under high temperature and pressure to lead the close-packed metals which induce the various degree of repulsion.

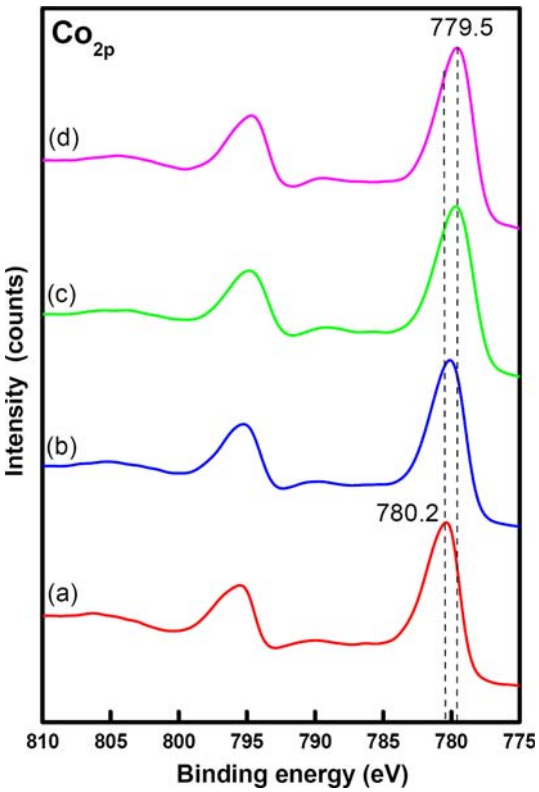

Fig. 4 XPS spectra of Co_{2p} of CeO_2–CoO_x catalysts: **a** IMP **b** PO **c** CP **d** HT

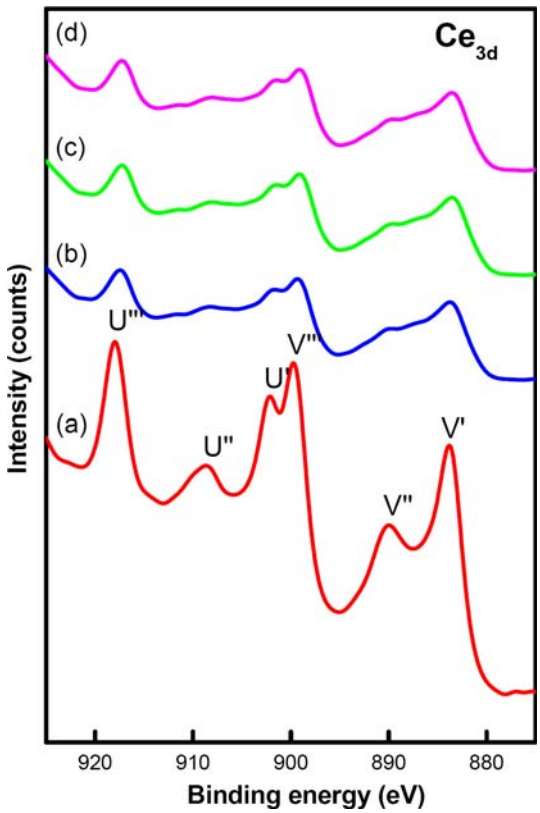

Fig. 5 XPS spectra of Ce_{3d} of CeO_2–CoO_x catalysts: **a** IMP **b** PO **c** CP **d** HT (V′, V″, V‴, U′, U″ and U‴ *labels* indicate the position of the Ce(IV)3d multiples)

Table 2 Analysis of surface composition of CeO_2–CoO_x

Sample	TEM–EDX (%)			XPS (%)			Ce_{3d}/Co^{a}_{2p}	Ce^{b}_{3d}	$Co_{2p3/2}$ (eV)
	Ce	Co	O	Ce	Co	O			
Co_3O_4 [29]	–	–	–	–	–	–	–	–	779.5
CoO [30]	–	–	–	–	–	–	–	–	780.5
IMP	20	43	37	21	41	38	0.49	0.8299	780.2
PO	19	39	42	5	53	42	0.09	0.1627	780.0
CP	19	44	37	5	52	44	0.07	0.1215	779.5
HT	18	45	37	4	53	43	0.06	0.1236	779.5

[a] Corrected for atomic sensitivity factor (area)

[b] Normalized peak area (a.u.)

To understand whether optimizing the preparation method can increase the surface area and maximize oxygen storage capacity, the ratio of α and β peaks from each CeO_2–CoO_x catalyst is quantitatively determined from the consumption of hydrogen, itself revealed by TPR traces under 300 °C. The relative areas of the α and β peaks (N_{H_2}/N_{Co}) of the IMP, PO, CP, and HT catalysts are determined to be 0.47:1.55; 0.46:1.39; 0.45:1.32, and 0.44:1.33, respectively. Also, Fig. 7 compares the degrees of reduction over CeO_2–CoO_x catalysts between 100 and 300 °C. Comparison with the theoretical values for Co_3O_4 (0.33:1 for α:β peaks) reveals that the amount of ceria on the surface can be released below 350 °C over these CeO_2–CoO_x catalysts. The higher surface area of binary catalyst and dispersion of ceria in the IMP sample is associated with a higher α:β ratio which reveals the effective oxygen-storage on ceria.

3.4 Oxidation of Carbon Monoxide

Figure 8 plots the catalytic activities of the CeO_2–CoO_x catalysts toward CO oxidation. Pure ceria is less active for CO oxidation so that the needed temperature exceeds 200 °C. The T_{50} (temperature at 50% CO conversion) of the IMP catalyst occurs at 88 °C, which is lower than other catalysts: the T_{50} values for the PO, CP and HT catalysts are 93, 103, and 119 °C, respectively. The IMP and PO catalysts are more active than the CP and HT catalysts. The IMP and PO catalysts possess higher surface area of 100 $m^2\ g^{-1}$ and a lower reduction temperature associated with the α peak than the other two catalysts. The IMP catalyst is more active than other catalysts. The superior catalytic performance of the IMP catalyst is related to the highest amount of well dispersed ceria that easily undergoes redox and strongly interacts with cobalt oxide. Based

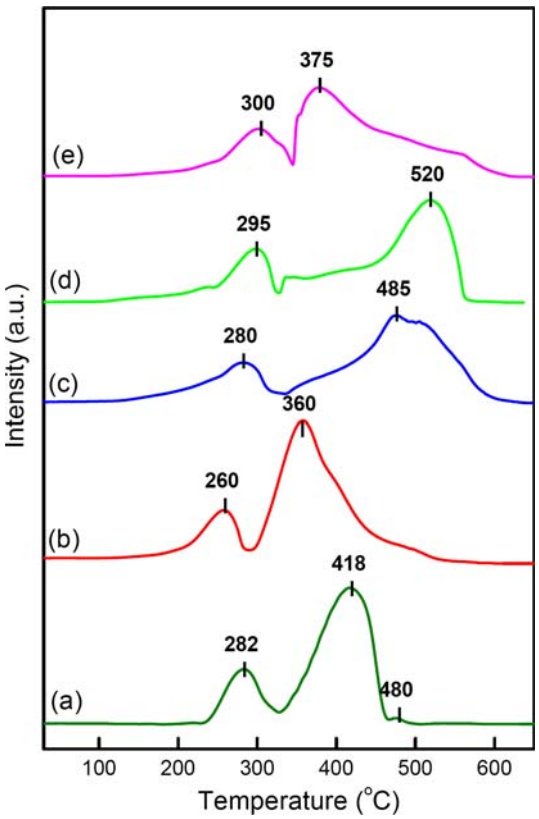

Fig. 6 TPR profiles of CeO_2–CoO_x catalysts: **a** PM **b** IMP **c** PO **d** CP **e** HT; the physically mixed catalyst assigned as PM

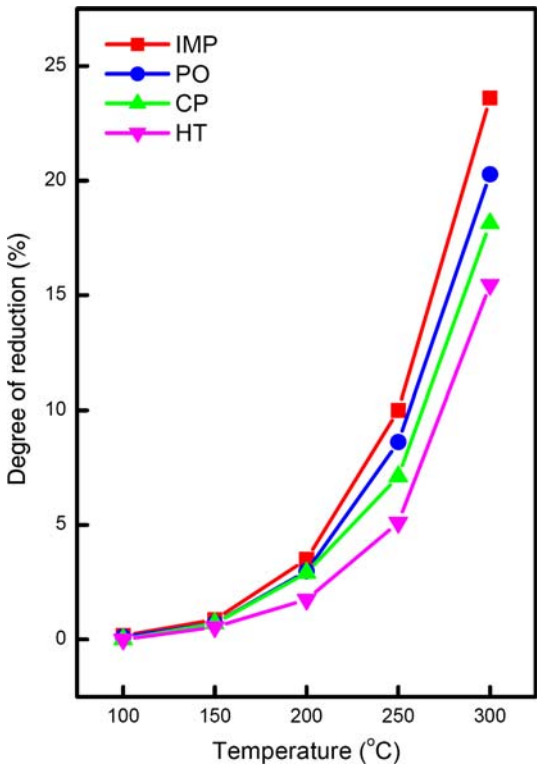

Fig. 7 Amounts of hydrogen consumption with the same temperature of CeO_2–CoO_x catalysts

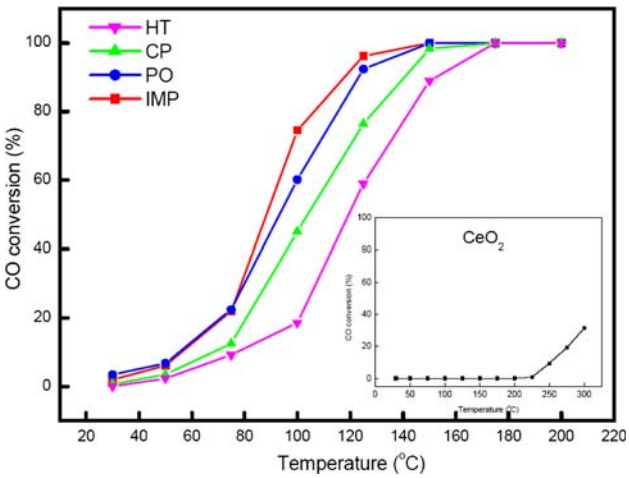

Fig. 8 Catalytic activity of CeO_2–CoO_x catalysts toward CO oxidation: **a** IMP **b** PO **c** CP **d** HT

on the characterization of catalysts three factors can influence the catalytic activities. First, the amount ceria on the surface of catalysts can be confirmed from the analysis of XPS. Second, the well-dispersion and high surface area of catalysts can be judged from the TEM and BET measurements. Third, the ability of reduction of catalysts can be analyzed by TPR. These factors are attributed to the method of preparation of catalysts which control the composition, surface area and dispersion of ceria. Therefore, better preparation method can promote the release of oxygen and thereby the oxidation of carbon oxide.

4 Conclusions

A comparison of the four various preparation methods prepared and used were IMP, CP, PO, and HT catalysts. The IMP catalyst was the most effective catalyst of the oxidation of CO, closely followed by the PO catalyst. The significant results of this study support the following conclusions.

1) The impregnation method yields well-dispersed ceria that strongly interacts with the cobalt oxide.
2) The precipitation oxidation method yields the highest surface area.
3) The activity in CO oxidation depends on both the surface area of the catalyst and the dispersion of ceria.

Acknowledgments We are pleased to acknowledge financial supports for this study from Academia Sinica and the National Science Council of the Republic of China.

References

1. Usmen RK, Graham GW, Watkins WLH, McCabe RW (1994) Catal Lett 30:53
2. Lamb AB, Bray C, Fraser JCW (1920) Ind Eng Chem 12:213
3. Trimm DL (1983) Appl Catal 7(3):249
4. Haruta M (1997) Catal Today 36:153
5. Kang M, Song MW, Lee CH (2003) Appl Catal A Gen 251:143
6. Tang X, Zhang B, Li Y, Xu Y, Xin Q, Shen W (2004) Catal Today 93/95:191
7. Park JW, Jeong JH, Yoon WL, Jung H, Lee HT, Lee DK, Park YK, Rhee YW (2004) Appl Catal A Gen 274:25
8. Jansson J (2000) J Catal 194:55
9. Mohamed MM, Katib SMA (2005) Appl Catal A Gen 287:236
10. Thammachart M, Meeyoo V, Risksomboon T, Osuwan S (2001) Catal Today 68:53
11. Lin R, Luoa MF, Zhong YJ, Yan ZL, Liu GY, Liu WP (2003) Appl Catal A Gen 255:331
12. Jansson J, Palmqvist AEC, Fridell E, Skoglundh M, Sterlund LO, Thormahlen P, Langer V (2002) J Catal 211:387
13. Lin HK, Wang CB, Chiu HC, Chien SH (2003) Catal Lett 86:63
14. Lin HK, Chiu HC, Tsai HC, Chien SH, Wang CB (2003) Catal Lett 88:169
15. Wang CB, Tang CW, Gau SJ, Chien SH (2005) Catal Lett 101:59
16. Broqvist P, Panas I, Person H (2002) J Catal 210:198
17. Liou YH, Loa SL, Lin CJ, Kuan WH, Weng SC (2005) J Hazard Mater B127:102
18. Haneda M, Kintaichi Y, Bion N, Hamada H (2003) Appl Catal B Environ 46:473
19. Bensalem A, Bozon-Verduraz F, Delamar M, Bugli G (1995) Appl Catal A Gen 121:81
20. Zamar F, Trovarelli A, De Leitenburg C, Dolcetti G (1995) J Chem Soc Chem Commun 965
21. Jiang XY, Lu GL, Zhou RX, Mao JX, Chen Y, Zheng XM (2001) Appl Sur Sci 173:208
22. Shiau CY, Ma MW, Chuang CS (2006) Appl Catal A Gen 301:89–95
23. Avgouropoulos G, Ioannides T, Matralis H (2005) Appl Catal B Environ 56:87
24. Shao JJ, Zhang P, Tang XF, Zhang BC, Song W, Xu YD, Shen WJ (2006) Chin J Catal 27:937
25. Shao JJ, Zhang P, Tang XF, Zhang BC, Liu JL, Xu YD, Shen WJ (2007) Chin J Catal 28:163
26. Tang X, Li Y, Huang X, Xu Y, Zhu H, Wang J (2006) Appl Catal B Environ 62:265
27. Tang CW, Kuo CC, Kuo MC, Wang CB, Chien SH (2006) Appl Catal A Gen 309:37
28. Tang CW, Kuo MC, Lin CJ, Wang CB, Chien SH (2008) Catal Today 131:520
29. Sinha ASK, Shanker V (1993) Ind Eng Chem Res 32:1061
30. Petrosius SC, Drago RS, Young V, Grunewald GC (1993) J Am Chem Soc 115:6131
31. Mullins DR, Overbury SH, Huntley DR (1998) Surf Sci 409:307
32. Burroughs P, Hamnett A, Orchard AF, Thornton G (1976) J Chem Soc Dalton Trans 17:1686
33. Paryjczak T, Rynkowski J, Karski S (1980) J Chromatogr 188:254
34. Brown R, Cooper ME, Whan DA (1982) Appl Catal 3:177
35. Trovarelli A (1996) Catal Rev Sci Eng 38:439